Vol. 15(2), pp. 53-66, July-December, 2023
DOI: 10.5897/JETR2023.0748
Article Number: 379653F71505
ISSN: 2006-9790
Copyright ©2023
Author(s) retain the copyright of this article
http://www.academicjournals.org/JETR

ACADEMIC JOURNALS
expand your knowledge

Journal of Engineering and Technology Research

Full Length Research Paper

Optimal support spacing for composite oil and gas pipelines

Olalekan Olaosebikan

Department of Mechanical Engineering, Elizade University, Ondo State, Nigeria.

Received 21 September, 2023; Accepted 26 October, 2023

Problems of premature breakage or failure may be encountered with composite pipelines used in the transportation of oil and gas products due to the manner in which these lines are laid or installed, especially in cases where the lines traverse long distances with rapidly varying topograghy over which considerable twisting and bending of the pipelines may occur. To overcome such problems, an analytical model is developed herein for determining the optimal spacings between successive supports of a transporting composite pipeline which would be effective in eliminating or minimizing the risk of failure or breakage of the line and at the same time substantially reducing the costs involved in excessive conservatism in existing specifications for this purpose. These dual benefits can be achieved through design specification on pipeline support spacing proposed in this paper which is simple and easy to use by pipeline operators and oil and gas exporting countries.

Key words: Pipelines, oil and gas, composite material, optimal support spacing, cylindrical shell theory, analytical solution, Excel calculations.

INTRODUCTION

Certain problems of premature failure or breakage encountered in the field application of composite pipes for the transportation of oil and gas products have been attributed to the manner in which these lines are laid or installed, especially in situations where the pipelines traverse long distances with rapidly varying topograghy (Figure 1). To overcome such problems, it is proposed to develop an analytical model for determining the optimal spacing between successive supports of a composite pipeline which would be efficient and cost-effective in eliminating or minimizing the risk of failure of a line during the transmission of oil and gas products.

In this report, the thin shell theory for anisotropic linearly elastic materials is used to model a composite pipeline's response to internal pressure and/or external loadings. Thereafter, an interactive failure criterion in stress or strain space is used to determine the optimal support spacing such that the pipeline would be safe from failure. It is found that the optimal spacing is not only a function of the pipe diameter, but also depends on the material of the pipe, the operating pressure of the line, the transported fluid, as well as the pipe cross-section geometry characterised by the ratio (D/h) of the diameter to the wall thickness. Specifications for support spacings contained in other models (SIPM, 1993), which are only expressed in terms of pipeline diameters, are found to be

E-mail: olalekan.olaosebikan@elizadeuniversity.edu.ng, lekan.ola1100@gmail.com.

Figure 1. Illustration of pipeline support spacing.

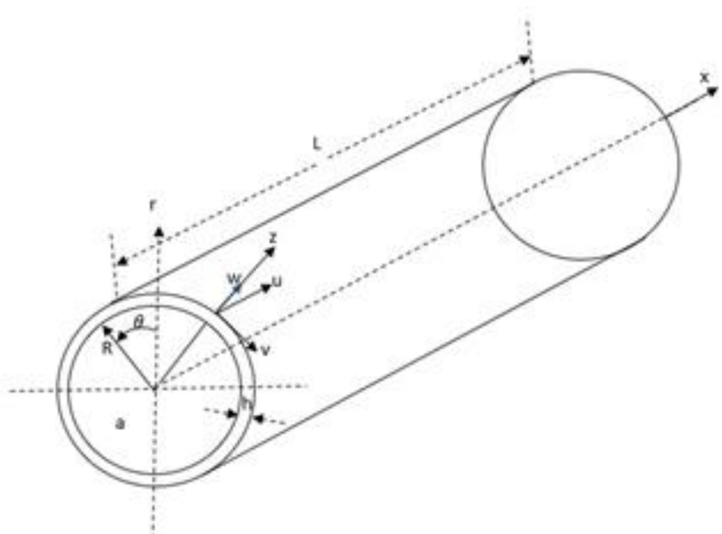

Figure 2a. Geometry of cylindrical shell model.

grossly inadequate.

PROBLEM FORMULATION

Pressure p and thrust P are axisymmetric, while q is uniformly distributed over the pipeline length. The coordinates and notations used here are shown in Figure 2a, and the supports and loadings are sketched in Figure 2b. The loadings comprise: internal pressure, p; weight loading (uniformly distributed), q; axial thrust, P. The key variable is the lateral deflection w(x), which in view of the combination of loads, and subject to the assumption of linear elastic response can be expressed as a superposition of two solutions as shown in Equation 1:

$$w(x) = w_{axi}(x) + w_{udl}(x) \tag{1}$$

where $w_{axi}(x)$ is the deflection under the axisymmetric loads, and $w_{udl}(x)$ is the deflection under the uniformly distributed loading.

The axisymmetric solution $w_{axi}(x)$ is determined from the differential equations for a thin shell of a linearly elastic anisotropic (but homogeneous) material. The solution for the uniformly distributed load $w_{udl}(x)$ is obtained approximately by use of simple beam theory. The strain (and stress) components, ε_{ij} (σ_{ij}), are found from the displacement components {u(x), v(x), w(x)} by use of standard kinematic and constitutive (stress-strain)

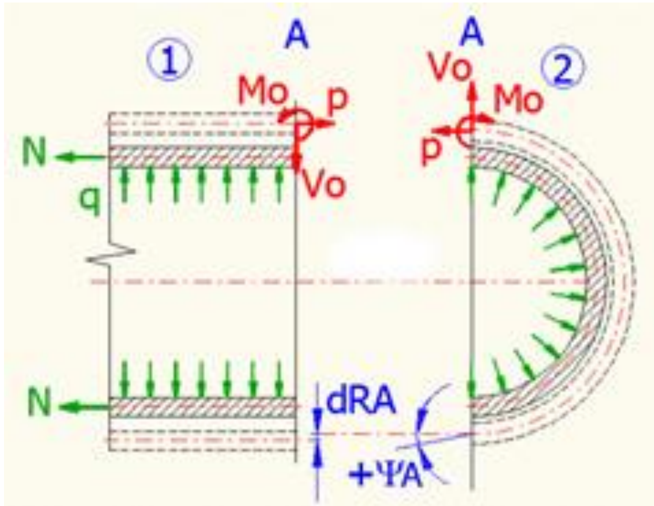

Figure 2b. Forces and moments (Note: alternative notations are in the Text).

relations.

A failure criterion is then applied at the most highly strained / stressed (that is the critical) part along the length of the pipeline. For a typical pipe segment on simple supports under the loadings specified above, the critical location is the inner surface at mid-span between the supports. The selected failure criterion is the Tsai-Wu interaction criterion in strain or stress space;Tsai SW, Hahn HT (1974) as shown in Equation 2 and 3:

$$G_{ij}\varepsilon_i\varepsilon_j + G_i\varepsilon_i = 1 \quad (2)$$

$$F_{ij}\sigma_i\sigma_j + F_i\sigma_i = 1 \quad (3)$$

The choice of this criterion is influenced both by the analytical basis from which it is derived for modelling the response of various types of composite stuctures to various loads, as well as by its widespread use and successful application to a variety of problems (Tsai and Hahn, 1974). The predictions of this criterion are compared with a simpler one of maximum strain / stress in this text. Following the determination of the strain / stress components from the displacement components w(x) and u_o(x), introduction of the failure criterion leads to a transcendential equation for finding the desired pipeline support length L which appears as a non-dimensional parameter α: $\alpha \equiv \varepsilon L/2$. The transcendential equation takes the form:

$$G_{cr}(\alpha) = 0 \quad (4)$$

whose roots (α) can be found numerically for specific data, for example by computation in an EXCEL spreadsheet or with a FORTRAN program. Sample results obtained from an EXCEL spreadsheet are shown and discussed

AXISYMMETRIC SOLUTION

General features

The axisymmetric solution w_{axi}(x) is determined from the differential equations for a thin shell of a linearly elastic anisotropic (but homogeneous) material, which may be written in the forms (Vinson, 1993) as shown in Equation 5:

$$\frac{d^4w}{dx^4} + 4\varepsilon^4 w = \frac{1}{D_x}\left(p(x) - \frac{\nu_{\theta x}}{R}N_x\right)$$
$$\frac{du_o}{dx} = \frac{N_x}{K_x} - \frac{\nu_{\theta x}}{R}w \quad (5)$$

where w(x) is the lateral deflection, u_o(x) is the mid-plane displacement, and the loading and geometric parameters are as shown in Figures 2a and 2b.

Since this pair of equations in w and u_o is uncoupled, the first of it alone is used to determine w_{axi}(x) as described subsequently. The pipeline is represented as a thin-walled circular cylindrical shell with uniform wall-thickness h, and radius R, taken to its midplane. The material of the shell is modelled as a specially orthotropic material, so that the material parameters contained in the governing Equation (5) are defined as followsas shown in Equation 6:

$$\varepsilon^4 \equiv \frac{3(1-\nu_{x\theta}\nu_{\theta x})}{h^2R^2}\frac{D_\theta}{D_x} \tag{6}$$

where $\nu_{x\theta}, \nu_{\theta x}$ are poisson's ratios w.r.t. the longitudinal and transverse directions respectively. (Equation 7):

$$D_\theta \equiv \frac{E_\theta h^3}{12(1-\nu_{x\theta}\nu_{\theta x})} \ , \ D_x \equiv \frac{E_x h^3}{12(1-\nu_{x\theta}\nu_{\theta x})} \ , \ K_x \equiv \frac{E_x h}{(1-\nu_{x\theta}\nu_{\theta x})} \tag{7}$$

The axisymmetric loading consists of an internal pressure p(x) together with an axial thrust N_x. The axial thrust N_x satisfies the condition (Equation 8):

$$\frac{dN_x}{dx} = 0 \tag{8}$$

so that N_x is a constant.

Also, for the present purpose, we take the pressure p(x) as a constant. This follows from the consideration that the internal pressure in pipelines varies little even over long distances. Typically, one gets a pressure drop of only 0.1 bar over a pipe length of 20 km (Vinson, 1974). The general solution to Equation 9 is the sum of a homogeneous solution $w_h(x)$, and a particular integral $w_p(x)$:

$$w(x) = w_{axi}(x) = w_h(x) + w_p(x) \tag{9}$$

For the particular integral $w_p(x)$, we observe that for N_x constant, and p(x) assumed a constant p, as shown in Equation 10:

$$w_p(x) = \frac{1}{4\varepsilon^4 D_x}\left(p - \frac{\nu_{\theta x}N_x}{R}\right) \tag{10}$$

In this expression, the pressure p will normally be prescribed from the operating conditions of a specific pipeline, while the axial thrust N_x is determined by the weight loading on the line.

The homogeneous solution $w_h(x)$ in Equation 9 can be expressed in the form (Vinson, 1993):

$$w_h(x) = Ae^{-\varepsilon x}\cos\varepsilon x + Be^{-\varepsilon x}\sin\varepsilon x + Ce^{\varepsilon x}\cos\varepsilon x + De^{\varepsilon x}\sin\varepsilon x \tag{11}$$

where the constants A, B, C, D are determined by applying appropriate boundary conditions for the problem to the general solution w(x). In Equation 11 and related ones following, notational equivalents used: $\varepsilon x \equiv \varepsilon_x$ to maintain the use in Vinson (1993).

The particular integral

The particular integral (Equation 10) is completely determined once N_x is found. To determine N_x, assume the pipe is resting on a series of simple supports which are equally spaced as illustrated in Figure 1. Then, a representative segment SG of length L between supports will experience an axial force P (Figures 3 and 2b) induced by weight loadings from the adjoining pipe segments on both sides of SG such that by symmetry and for balance of moments about either support, we have (Equation 12):

$$PR = \frac{W}{2}\frac{L}{4} \text{ , so that } P = \frac{WL}{8R} \tag{12}$$

where W is the total weight loading on any pipe segment, as typified by SG. Here, W is the sum of the weight of the pipe W_p and that of the fluid W_f instantaneously contained within its length. Under steady flow conditions, we have (Equation 13):

$$W = W_p + W_f \tag{13}$$

Let the specific gravity of the pipe material be s_p, and that of the contained fluid s_f. Then for this shell geometry we find that in Equation 14:

$$\begin{aligned} W = W_p + W_f &= 2\pi RhLs_p\rho_w + \pi R^2 Ls_f\rho_w \\ &= \rho_w \pi RL(2hs_p + Rs_f) \end{aligned} \tag{14}$$

where ρ_w is the specific weight of water, that is ρ_w = 9.81E-06 N/mm^3.

By definition, the axial thrust N_x is obtained from the axial force P through the relation (Equation 15):

$$N_x = \frac{P}{2\pi R} = \frac{1}{2\pi R}\left(\frac{WL}{8R}\right) = \frac{WL}{16\pi R^2} \tag{15}$$

Consequently, on using Equations 12 - 15, we find that the particular integral given Equation 10 takes the form (Equation 16):

$$w_p = \frac{1}{4\varepsilon^4 D_x}\left(p - \frac{\nu_{\theta x}}{R}\frac{L}{16\pi R^2}\rho_w \pi RL(2hs_p + Rs_f)\right) \tag{16}$$

The general solution

The general solution (Equation 9) is completely

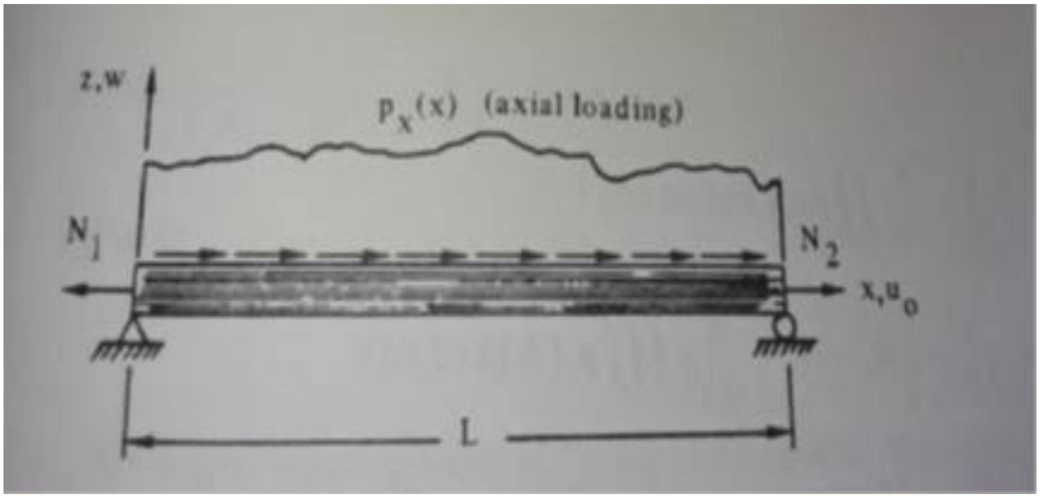

Figure 3. Model of a simply supported beam under external distributed load and internal pressure.

determined once the constants A, B, C, and D in the homogeneous solution (Equation 11) have been found by applying appropriate boundary conditions to the general solution w(x) in Equation 9. Consider again a typical pipe segment SG of length L between simple supports at S and G (Figures 1 and 3). Set the origin of axial coordinate x at midspan O, so that by symmetry, only one-half of this segment needs to be considered. The appropriate boundary conditions are (Equation 17):

$$w'(x)\big|_{x=0}=0\ , \qquad w'''(x)\big|_{x=0}=0$$
$$w(x)\big|_{x=\pm L/2}=0\ , \qquad w''(x)\big|_{x=\pm L/2}=0 \qquad (17)$$

We write the general solution w(x) as (Equation 18):

$$w(x)=w_p+Ae^{-\varepsilon x}\cos\varepsilon x+Be^{-\varepsilon x}\sin\varepsilon x+Ce^{\varepsilon x}\cos\varepsilon x+De^{\varepsilon x}\sin\varepsilon x \qquad (18)$$

Then by successive differentiation, we find (Equation 19):

$$w'(x)=-A\varepsilon e^{-\varepsilon x}(\sin\varepsilon x+\cos\varepsilon x)+B\varepsilon e^{-\varepsilon x}(\cos\varepsilon x-\sin\varepsilon x)$$
$$+C\varepsilon e^{-\varepsilon x}(-\sin\varepsilon x+\cos\varepsilon x)+D\varepsilon e^{-\varepsilon x}(\cos\varepsilon x+\sin\varepsilon x) \qquad (19)$$

$$w''(x)=2\varepsilon^2\left\{Ae^{-\varepsilon x}\sin\varepsilon x-Be^{-\varepsilon x}\cos\varepsilon x-Ce^{\varepsilon x}\sin\varepsilon x+De^{\varepsilon x}\cos\varepsilon x\right\} \qquad (20)$$

$$w'''(x)=2\varepsilon^3e^{-\varepsilon x}\left\{A(\cos\varepsilon x-\sin\varepsilon x)+B(\sin\varepsilon x+\cos\varepsilon x)\right\}$$
$$-2\varepsilon^3e^{\varepsilon x}\left\{C(\cos\varepsilon x+\sin\varepsilon x)+D(\sin\varepsilon x-\cos\varepsilon x)\right\} \qquad (21)$$

Conditions $(3.13)_1$ at x=0 yield (Equation 22):

$$-A+B+C+D=0$$
$$A+B-C+D=0 \qquad (22)$$

while conditions $(3.13)_2$ at x=L/2 yield (Equation 23):

$$Ae^{-\alpha}\cos\alpha+Be^{-\alpha}\sin\alpha+Ce^{\alpha}\cos\alpha+De^{\alpha}\sin\alpha=-w_p$$
$$Ae^{-\alpha}\sin\alpha-Be^{-\alpha}\cos\alpha-Ce^{\alpha}\sin\alpha+De^{\alpha}\cos\alpha=0 \qquad (23)$$

where, $\alpha\equiv\varepsilon L/2$.

Equation 22 lead to the relations

$$C=A\ , \quad \text{and} \quad D=-B \qquad (24)$$

which are subsequently used in Equation 23 to obtain the results (Equation 25):

$$A=C=-w_p g(\alpha)$$
$$B=-D=w_p t(\alpha)g(\alpha) \qquad (25)$$

where,

$$g(\alpha)\equiv\ 2\cos\alpha\cosh\alpha(1+\tan^2\alpha\tanh^2\alpha)^{-1}$$
$$t(\alpha)\equiv\tan(\alpha)\tanh(\alpha)$$

so that the constants A, B, C, and D are functions of the parameter $\alpha \equiv \varepsilon L/2$.

SOLUTION FOR THE UNIFORMLY DISTRIBUTED LOAD

An approximate solution for the lateral deflection of the pipeline under the uniformly distributed weight loading can be constucted by regarding the typical pipe segment as a simply-supported beam of length L, carrying the said loading along its length, Figure 3. The use of simple beam theory is illustrated in Figure 3. Here, the origin of the axial coordinate is placed at midspan as for the axisymmetric problem.

Let the load per unit pipe length be q. Then by relation (11), we have Equation 26:

$$q = \frac{W}{L} = \rho_w \pi R\left(2hs_p + Rs_f\right) = 9.81*10^{-6}\pi R^2\left(2\frac{h}{R}s_p + s_f\right) \quad (26)$$

Then from the free-body-diagram in Figure 2b, we find that the bending moment M(x) is given in Equation 27:

$$M + qL\left(\frac{L}{2}-x\right) = q\left(\frac{L}{2}-x\right)\frac{1}{2}\left(\frac{L}{2}-x\right) \quad (27)$$

so that the equation for flexural deflection is

$$EIw''(x) = M(x) = \frac{q}{2}\left(\frac{L}{2}-x\right)^2 - qL\left(\frac{L}{2}-x\right)$$

where the flexural rigidity EI is taken with respect to the pipe axis, that is $EI = E_x I_x$, and $E = E_x$ is Young's modulus w.r.t. the axial direction, while $I = I_x$ is the second moment of area of the pipe cross-section w.r.t. the pipe axis, which for a thin circular cylindrical shell of mid-radius R and wall thickness h is given (Equation 28):

$$I_x = (\text{pipe cross-section area}) * R^2 = 2\pi R^3 h \quad (28)$$

For convenience, we drop the subscript x on E and I as there would be no ambiguity in doing so here. Integrating (Equation 27)$_2$, we obtain successively (Equation 28):

$$\frac{2EI}{q}w'(x) = -\frac{1}{3}\left(\frac{L}{2}-x\right)^3 + L\left(\frac{L}{2}-x\right)^2 + C_1$$
$$\frac{2EI}{q}w(x) = \frac{1}{12}\left(\frac{L}{2}-x\right)^4 - \frac{L}{3}\left(\frac{L}{2}-x\right)^3 + C_1 x + C_2 \quad (29)$$

where C_1 and C_2 are constants of integration which are evaluated from the following boundary conditions for a simply-supported pipe-beam (Equation 30):

$$w'(x)\big|_{x=0} = 0 \ , \quad w(x)\big|_{x=L/2} = 0$$

from which we obtain

$$C_1 = -\frac{5}{24}L^3 \ , \quad C_2 = \frac{5}{48}L^4$$

Consequently, the lateral deflection w_{udl} under the uniformly distributed load is given in Equation 31:

$$w_{udl}(x) = \frac{q}{48EI}\left\{2\left(\frac{L}{2}-x\right)^4 - 8L\left(\frac{L}{2}-x\right)^3 + 5L^3\left(\frac{L}{2}-x\right)\right\}$$

or, alternatively:

$$w_{udl}(x) = \frac{qL^4}{48EI}\left\{2\left(\frac{1}{2}-\frac{x}{L}\right)^4 - 8\left(\frac{1}{2}-\frac{x}{L}\right)^3 + 5\left(\frac{1}{2}-\frac{x}{L}\right)\right\} \quad (31)$$

COMBINED SOLUTION

Total lateral deflection

By superposition, as explained previously (Equation 1), the total lateral deflection of the pipe under the combination of the axisymmetric and uniformly distributed loads is (Equation 32):

$$w(x) = w_{axi}(x) + w_{udl}(x)$$
$$= w_p + 2A\cos\varepsilon x\cosh\varepsilon x - 2B\sin\varepsilon x\sinh\varepsilon x + \kappa\left\{2\left(\frac{1}{2}-\frac{x}{L}\right)^4 - 8\left(\frac{1}{2}-\frac{x}{L}\right)^3 + 5\left(\frac{1}{2}-\frac{x}{L}\right)\right\} \quad (32)$$

where w_p is given Equation 15, A and B by Equation 24, and for convenience we have set (Equation 33):

$$\kappa = \frac{qL^4}{48E_x I_x} = \frac{q}{3E_x I_x}\frac{\alpha^4}{\varepsilon^4} \quad (33)$$

the last step following from the relation $\alpha \equiv \varepsilon L/2$.

Strain components

The total lateral deflection w(x) obtained in Equation 32 is independent of the circumferential coordinate θ, so that the strain components w.r.t. the (x, θ) plane are given:

$$\varepsilon_x = \frac{du_o}{dx} - \varsigma\frac{d^2 w}{dx^2} \ , \quad \varepsilon_\theta = \frac{w(x)}{R} \ , \quad \varepsilon_{\theta x} = 0 \quad (34)$$

Where ς is the radial coordinate measured from the pipe mid-surface.

As the shear component $\varepsilon_{\theta x}$ is zero, ε_x and ε_θ become the principal strain components in the pipe wall. This feature is utilized subsequently. Substituting Equation 5 ($_2$) in 33 ($_1$) leads to Equation 35:

$$\varepsilon_x = \frac{N_x}{K_x} - \frac{\nu_{\theta x}}{R} w(x) - \varsigma w''(x) \tag{35}$$

Hence from the expression obtained for w(x) in Equation 32, together with Equations 16, 25, and 8, the strain components ε_x and ε_θ can be calculated using Equations 35 and 34($_2$). For this, we observe that w''(x) resulting from Equation 32 is:

$$w''(x) = 4\varepsilon^2 g(\alpha) w_p \{\sin \varepsilon_x \sinh \varepsilon_x - t(\alpha)\cos\varepsilon_x \cosh\varepsilon_x\} + \frac{24\kappa}{L^2}\left\{\left(\frac{1}{2}-\frac{x}{L}\right)^2 - 2\left(\frac{1}{2}-\frac{x}{L}\right)\right\} \tag{36}$$

The use of Equations 32 and 36 in Equations 34 and 35 give the final expressions for $\varepsilon_x(x)$ and $\varepsilon_\theta(x)$ in terms of the quantities w_p, g(α), t(α), ε_x, and (1/2 - x/L). Only the reduced forms of these expression obtained for a specific value of variables (x, ζ) are needed in the application of the failure criterion, and these are written out explicitly in the following where the failure criterion is discussed.

APPLICATION OF A FAILURE CRITERION

Interactive failure criterion

The selected failure criterion is the Tsai-Wu interactive criterion in either strain or stress space, expressed by Equations 2. Note that the strain- and stress- space expressions are equivalent, the use of one rather than the other is determined in specific cases by the data available for the computation involved. An EXCEL spreadsheet can be written to allow the use of either form of this criterion. To use the stress-space form, the stress components are first calculated from the strain components, using the stress-strain relations Equation (37):

$$\sigma_\theta = \frac{1}{(1-\nu_{x\theta}\nu_{\theta x})}\left(E_\theta\varepsilon_\theta + \nu_{\theta x}E_x\varepsilon_x\right)$$
$$\sigma_x = \frac{1}{(1-\nu_{x\theta}\nu_{\theta x})}\left(E_x\varepsilon_x + \nu_{x\theta}E_\theta\varepsilon_\theta\right) \tag{37}$$

The said criterion is applied at the most highly strained / stressed region in the pipe. For the problem being investigated, this critical region is the inner surface of the pipe at its midspan, that is at x = 0 and ζ = -h/2. Set

$$\varepsilon_x\Big|_{x=0,\ \varsigma=-h/2} = \hat{\varepsilon}_x \ , \ \varepsilon_\theta\Big|_{x=0} = \hat{\varepsilon}_\theta \ , \ \varepsilon_{x\theta} \equiv 0 \tag{38}$$

Then from previous section (The total lateral deflection), we found:

$$\hat{\varepsilon}_x = \frac{N_x}{K_x} - \frac{\nu_{\theta x}}{R}\left(w_p(1-2g(\alpha)) + \frac{13}{8}\kappa\right) - 2h\varepsilon^2\left(w_p g(\alpha)t(\alpha) + \frac{9}{8}\frac{\kappa}{\alpha^2}\right)$$
$$\hat{\varepsilon}_\theta = \frac{1}{R}\left(w_p(1-2g(\alpha)) + \frac{13}{8}\kappa\right) \tag{39}$$

The strain-space criterion $(2.2)_1$ can be expanded into [4]

$$G_{11}\varepsilon_1{}^2 + 2G_{12}\varepsilon_1\varepsilon_2 + 2G_{22}\varepsilon_2{}^2 + G_{ss}\varepsilon_s{}^2 + G_1\varepsilon_1 + G_2\varepsilon_2 - 1 = 0$$

and correspondingly for the stress space, we have

$$F_{11}\sigma_1{}^2 + 2F_{12}\sigma_1\sigma_2 + 2F_{22}\sigma_2{}^2 + F_{ss}\sigma_s{}^2 + F_1\sigma_1 + F_2\sigma_2 - 1 = 0$$

where subscript 1 denotes the fiber direction, 2 the direction normal to that of the fibers, and s the shear component. For the pipe geometry here, (Figure 2a), the fiber direction is the circumferential (or θ-) direction, while the axial (or x-) direction is the one normal to the fibers. This follows from the manner in which fiber-reinforced materials are wound into circular pipe profiles.

Furthermore, at the critical region where the criterion is being applied the shear strain component vanishes. Hence in Equations 40 and 41, we set Equation 42:

$$\varepsilon_1 = \hat{\varepsilon}_\theta \ , \ \varepsilon_2 = \hat{\varepsilon}_x \ , \ \varepsilon_s \equiv 0$$

Then substituting Equation 39 Equations in 40 and 41 leads to a transcendential equation of the form Equation 4 for determining the values of α ≡ εL/2, which satisfy the failure criterion Equation 2. Thereafter, from the set of values of L resulting from the solution of this transcendential equation the required optimal support spacing can be extracted. This is explained further subsequently.

Dimensionless form

To make the dependence of the required quantity L (or α) on the governing parameters more apparent, we re-arrange the variables occurring in the failure criterion (Equations 40 and 41) in non-dimensional form. To this end, we rewrite the expressions for the strain components ε_1 and ε_2 as follows in Equation 43:

$$\varepsilon_1 = \hat{\varepsilon}_x = \frac{N_x}{K_x} - \nu_{\theta x}\left(\frac{w_p}{R}(1-2g(\alpha)) + \frac{13}{8}\frac{\kappa}{R}\right) - 2h\varepsilon^2\left(w_p g(\alpha)t(\alpha) + \frac{9}{8}\frac{\kappa}{\alpha^2}\right)$$
$$\varepsilon_2 = \hat{\varepsilon}_\theta = \frac{w_p}{R}(1-2g(\alpha)) + \frac{13}{8}\frac{\kappa}{R} \quad (43)$$

Note that the last term in the expression for ε_1 can be rewritten as in Equation 44:

$$2h\varepsilon^2\left(w_p g(\alpha)t(\alpha) + \frac{9}{8}\frac{\kappa}{\alpha^2}\right) = 2h\frac{\delta}{hR}\left(w_p g(\alpha)t(\alpha) + \frac{9}{8}\frac{\kappa}{\alpha^2}\right) = 2\delta\left(\frac{w_p}{R} g(\alpha)t(\alpha) + \frac{9}{8}\frac{\kappa}{R\alpha^2}\right) \quad (44)$$

Hence from (6.6) and (6.7) we see that the dimensionless variables which enter into Equations 40 and 41 are (as shown in Equation 45):

$$\alpha, \quad \frac{N_x}{K_x}, \quad \frac{w_p}{R}, \quad \frac{\kappa}{R}$$

of which α becomes the dependent variable and the rest, the specified or independent variables. Furthermore, we have the following relations (as shown in Equation 46):

$$\frac{N_x}{K_x} = \frac{\rho_w \alpha^2}{4\varepsilon^2}\left(2\frac{h}{R}s_p + s_f\right)\frac{(1-\nu_{x\theta}\nu_{\theta x})}{E_x h} = S_m \frac{E_\theta}{E_x}\frac{\nu_s}{4\delta}\frac{R}{h}\alpha^2$$

where

$$\varepsilon^2 \equiv \frac{\delta}{hR}, \text{ with } \delta \equiv \sqrt{3(1-\nu_{x\theta}\nu_{\theta x})E_\theta / E_x}, \; S_m \equiv \frac{\rho_w h}{E_\theta}\left(2\frac{h}{R}s_p + s_f\right), \; \nu_s \equiv (1-\nu_{x\theta}\nu_{\theta x}) \quad (46)$$

Similarly, using relations found earlier previously, we have (as shown in Equation 47):

$$\frac{w_p}{R} = \frac{1}{R}\frac{1}{4\varepsilon^4 D_x}\left(p - \frac{\nu_{\theta x}N_x}{R}\right) = \frac{1}{R}\frac{R^2}{hE_\theta}\left(p - \frac{\nu_{\theta x}N_x}{R}\right) = \frac{R}{h}\left(\frac{p}{E_\theta} - \frac{\nu_{\theta x}N_x}{RE_\theta}\right) = \frac{R}{h}\left(\frac{p}{E_\theta} - \nu_{\theta x}S_m\frac{\alpha^2}{4\delta}\right)$$
$$\frac{\kappa}{R} = \frac{1}{R}\left\{\rho_w\left(2\frac{h}{R}s_p + s_f\right)\frac{hR}{18\nu_s}\frac{\alpha^4}{E_\theta}\right\} = \frac{S_m\alpha^4}{18\nu_s} \quad (47)$$

Thus Equation 43 become Equation 48

$$\varepsilon_1 = \hat{\varepsilon}_x = S_m\frac{E_\theta}{E_x}\frac{\nu_s}{4\delta}\frac{R}{h}\alpha^2 - \nu_{\theta x}\varepsilon_2 - 2\delta\left(\frac{w_p}{R}g(\alpha)t(\alpha) + \frac{9}{8}\frac{S_m\alpha^2}{18\nu_s}\right)$$
$$\varepsilon_2 = \hat{\varepsilon}_\theta = \frac{w_p}{R}(1-2g(\alpha)) + \frac{13}{8}\frac{S_m\alpha^4}{18\nu_s} \quad (48)$$

Consequently, the transcendential equation for α resulting from (Equations 40 and 41), have the functional form in Equation 49:

$$G_{cr}\left(\alpha;\; \frac{R}{h}, \frac{p}{E_\theta}, S_m, \delta, \nu_s\right) \quad (49)$$

(49)

which gives the quantity $\alpha \equiv \varepsilon L/2$ as a function of the form (as shown in Equation 54):

$$\alpha = f\left(\frac{R}{h}, \frac{p}{E_\theta},\; S_m, \delta, \nu_s\right) \quad (50)$$

Thus we see that the required optimal support spacing L_{opt} to be extracted from Equation 50 is a function of the following variables or parameters:

1. Pipe cross-section geometry, represented by the variable R/h or D/h;
2. Pressure loading, represented by variable p/Eθ*;
3. Pipe material and fluid content, represented by parameters Sm, *, *s .

Because of the non-linear character of the dependence of L_{opt} on each of the variables in Equation 54, the features of these dependences cannot be expressed in a closed analytical form. However, they are displayed graphically and in tabular forms.

DISCUSSION

Features

Equation 49 is found to be a quartic equation in α^2 so that there could be up to 4 real roots for α^2. If there are any complex roots, they would occur in conjugate pairs in the resulting values for α . In fact, only 2 real roots have been detected for α^2 for a wide range of values of the main independent variables shown on the r.h.s of Equation 50. The range of values used are given in Tables 1.1 to 1.6 in Appendix I. Of the two roots of in Equation 49 only one can be considered acceptable as the other one gives a vanishingly small value for the

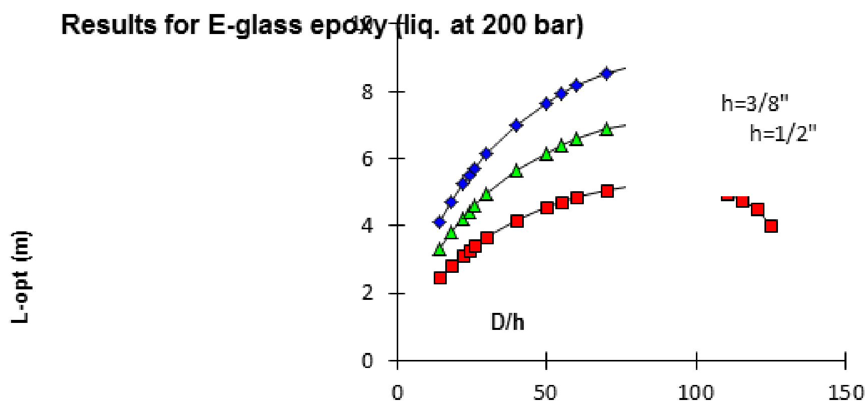

Figure 4. L_{opt} vs. D/h for varying h values, for E-glass epoxy.

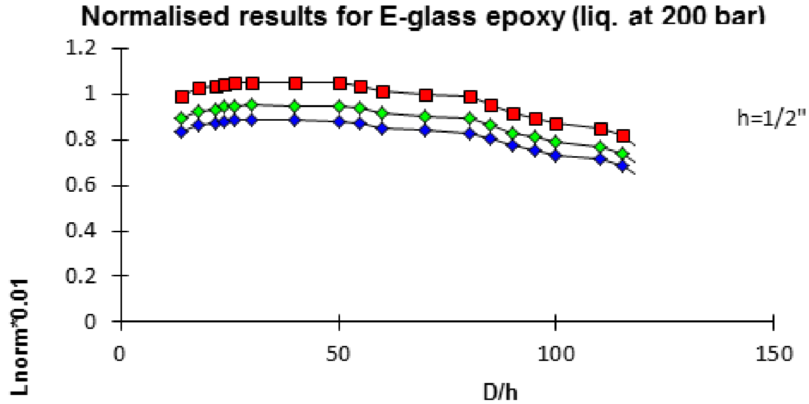

Figure 5. L_{opt} vs. D/h for a fixed h value, for graphite epoxy.

support spacing. Hence the solution can be considered sound as there would be no ambiguities for any specific case. This can be seen from the last four columns of the EXCEL printout shown as Appendix III (A)

Samples of the resulting solutions for ***optimal support spacing L_{opt}*** are shown graphically and in tabular form for various combinations of the governing variables (Figures 4 to 6):

1. Lopt vs. D/h, for various values of h, at constant pressure p;
2. Lopt vs. D/h, for various p, with h fixed;
3. Lopt vs. D/h, for different transported fluids, with h fixed.

A non-dimensional form of the graph of L_{opt} vs. D/h, for various h, at constant p, is the graph of Equation 51:

$$\frac{L_{opt}}{\sqrt{hD}}.vs.\frac{D}{h} \tag{51}$$

which shows other interesting features. For the non-dimensionalisation, it was observed in Equation 52 that:

$$\alpha \equiv \frac{\varepsilon L}{2} = c\frac{L_{opt}}{\sqrt{hD}},$$

where (52)

$$c = \sqrt{\frac{\delta}{2}}, \quad \text{with} \quad \delta \equiv \sqrt{3(1-\nu_{\theta x}\,\nu_{x\theta})E_\theta /\ E_x}$$

Sample results

The computed results for the sample calculations are shown in Tables 1 to 6 in Appendix I. The corresponding graphs are contained in Appendix II. The reference data for the calculations are also shown in Table 1 in Appendix I. Table 1 gives a comparison of the results with some existing solutions; Vinson JR, Sierakowski A (1986)

Scope of application

As illustrated in the examples, the solution for α ceases

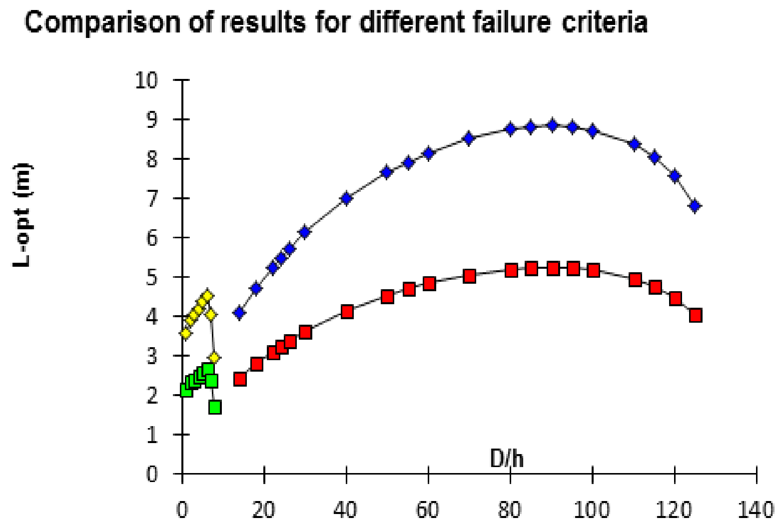

Figure 6. L_{opt} vs. D/h for gas-transmission lines.

to be acceptable when its value suddenly drops sharply for a minute increase in D/h (Figure 6). At this point it is found that the second real root gets very close to the first, both of which then become vanishingly small and therefore unacceptable.

This transition point marks the limit of validity of the foregoing solution and its point of occurrence is governed mainly by the applied pressure load for a given failure criterion and given material. Different limits are found for different criteria and different materials. A comparison of the limits set by different criteria is illustrated in Figure 6. For application of the model for D/h values beyond the range of validity, the terminal value in this range may be used, alternatively, a continuous foundation or support may become necessary, see for example the last column of Table 3.1b.

On the whole, the interaction failure criterion in strain or stress space seems to give the most reliable solutions, and may be regarded as an 'upper' bound criterion. Furthermore, the range of solutions that can be obtained would cover all cases of practical concern and analytical interest.

Application to other loading conditions

As indicated previously, the model developed here can be applied to other pipe loadings or configuration by an appropriate interpretation or modification of the governing variables. Thus, for application to offshore pipelines, the pressure p would be defined as shown in Equation 57:

$$p = p_i - po \quad (53)$$

where,

p_i is the internal pressure load as before, and

p_o is the external hydrostatic pressure: $p = \rho_w H_w$

For buried land pipes, the weight loading is redefined as shown in Equation 58:

$$W = W_p + W_f + W_s$$

Where W_p and W_f are as before and W_s is the weight of the 'head' of soil covering the pipe. That is,

$$W_S = \rho_S H_S LD$$

Conclusion

The interactive failure criterion for composites has been used to determine the optimal support spacing for composite pipelines. The analysis, based on thin shell theory, shows that the optimal support spacing depends on the following parameters: The pipe cross-section geometry (D/h), the pressure loading (p/Eo), the transported fluid type and the material properties of the pipeline. This result is a considerable improvement on some previous specification on pipe support, which is solely determined by the pipe diameter, and provides an excessively conservative estimate of spacing distances, and is only valid for a very limited range of application.

The interaction criterion is also compared with other criteria, such as the maximum strain criterion, and found to be much more reliable and found to cover a much wider scope of application.

Furthermore, although the formulation is initially for overland pipelines, by appropriate modification or interpretation of the input variables (such as inclusion of hydrostatic pressure head for offshore lines, etc.), the model can be applied directly to offshore and buried land pipes.

Recommendations

From the study, the following recommendations are made:

1. In the model discussed here, the pipe layout is assumed to be horizontal throughout its entire length, which can be extensive and include a large number of supports. A useful extension of the work could include varying slopes between supports, to account for possible variation in the land or surface topography.
2. The effect of field joints on the pipelines has not been included here. Where supports are placed at joint locations, the stress distribution over the representative pipe segment would be different and the failure criterion would need to be applied at the joints rather than at midspan as done here.
3. A simple composite structure has been used here, namely that of a single layer, unidirectional composite. This may be sufficient for an estimate of the required quantity, L_{opt}, in many practical cases, but it is worthwhile to investigate the difference, if any, it would make when one considers a multi-layered and multi-directional composite.
4. The Excel calculation should be developed into a *software* package for use in pipeline design and installation; Vinson JR, Sierakowski A (1986), Vinson and Chou (1975) and Mirsky (1964).

CONFLICT OF INTERESTS

The author has not declared any conflict of interests.

ACKNOWLEDGEMENT

This work was initiated at Shell-Billiton Research in Arnhem (BRA), The Netherlands when the author was visiting research scientist (1992-1994). Accordingly, the author gratefully acknowledges the opportunity and support by the Materials Characterisation Division.

REFERENCES

Mirsky I (1964). Axisymmetric vibrations of orhotropic cylinders, Journal of Acoustic Society of America 36:2106-2112.
SIPM (1993). Specifications and Recommended Practice for the use of GRP Piping Offshore: Part 3 - System Design. Shell International Draft Final Document.
Tsai SW, Hahn HT (1974). Introduction to composite materials. Technomic Publishing Co., Connecticut.
Vinson JR (1974). Structural Mechanics: The Behaviour of Plates and Shells, John Wiley and Sons.
Vinson JR (1993). The behaviour of shells composed of isotropic and composite materials. Kluwer Academic Publishers, Dordrecht, The Netherlands.
Vinson JR, Chou TW (1975). Composite materials and their use in Structures, Applied Science Publishers, London.
Vinson JR, Sierakowski A (1986). The behaviour of structures composed of composite materials, Martinus Nijhoff Publishers.

APPENDIX

Appendix I. Data used in the excel calculations.

(A). Properties of the sample pipe materials (cf. [2, 5])

Table 1a. Mean strength values (MPa).

Material	Long. tens. X	Long. comp. X'	Trans. tens. Y	Trans. comp. Y'	Shear, S
E-glass epoxy (EGE)	1323	1491.2	54.44	108.9	79
S-glass epoxy (SGE)	937.93	1931	27.586	137.93	41.38
Graphite-epoxy	1500	1500	40	246	68

Table 2a. Strength parameters in stress space.

Material	F_{xx} (GPa)$^{-2}$	F_{yy} (GPa)$^{-2}$	F_{xy} (GPa)$^{-2}$	F_{ss} (GPa)$^{-2}$	F_x (GPa)$^{-1}$	F_y (GPa)$^{-1}$
E-glass epoxy (EGE)	0.50688	168.6763	-4.62327	160.2307	0.08526	9.1861
S-glass epoxy (SGE)	0.55214	262.8164	-6.0231	584.0083	0.5483	29.0
Graphite-epoxy	0.444	101.6	-3.36	216.2	0	20.93

Table 3a. Strength parameters in strain space (dimensionless) - see [4] for formulae for calculating these quantities from the F-values.

Material	G_{xx}	G_{yy}	G_{xy}	G_{ss}	G_x	G_y
E-glass epoxy	790.302	11712.24	1590.64	2746.29	23.383	77.276
S-glass epoxy	1068.7	18291.07	2851.65	10009.67	84.7494	244.564
Graphite-epoxy	12004	10680	-3069	11117	60.64	216.5

Table 4a. Engineering constants and specific gravity.

Material	E_x (GPa)	E_y (GPa)	υ_{xy}	υ_{yx}*	E_s (GPa)	Sp. gr.
E-glass epoxy	11.69	19.03	0.42144	0.68613	11.8354	1.8
S-glass epoxy	58.07	13.793	0.293	0.067	5.31	1.7
Graphite-epoxy	181	10.3	0.28		7.17	1.6

* $\upsilon_{xy}/E_x = \upsilon_{yx}/E_y$.

(B). Specific gravity (s.g.) of transported fluids

Table 1b. Specific gravities of selected fluids.

Fluid	Specific gravity (s.g.)
Water	1.0
Crude oil	0.9
Natural gas	0.005

(C). Selected pipe geometries

Table 1c. Sample pipe geometries for oil and gas transportation.

Application	Nom. Diam., D (in)	Wall thick., h (in)	D/h range (typical)
Flowlines (F/L)	4, 6, 8	1/8, 1/4	16 - 64
Delivery lines (D/L)	10, 14, 16	1/4, 1/2	20 - 64
Trunk lines (T/L)	18, 20, 24	1/2 - 1	18 - 48
Loading lines (L/L)	30, 40, 50	1, 1.5, ..	20 - 50

Appendix II: Data used in the Excel Calculations
(A) Properties of the sample pipe materials (cf. [2, 5])

Table A.1. Mean strength values (MPa).

Material	Long. tens. X	Long. comp. X'	Trans. tens. Y	Trans. comp. Y'	Shear, S
E-glass epoxy (EGE)	1323	1491.2	54.44	108.9	79
S-glass epoxy (SGE)	937.93	1931	27.586	137.93	41.38
Graphite-epoxy	1500	1500	40	246	68

Table A.2. Strength parameters in stress space.

Material	F_{xx} (GPa)$^{-2}$	F_{yy} (GPa)$^{-2}$	F_{xy} (GPa)$^{-2}$	F_{ss} (GPa)$^{-2}$	F_x (GPa)$^{-1}$	F_y (GPa)$^{-1}$
E-glass epoxy (EGE)	0.50688	168.6763	-4.62327	160.2307	0.08526	9.1861
S-glass epoxy (SGE)	0.55214	262.8164	-6.0231	584.0083	0.5483	29.0
Graphite-epoxy	0.444	101.6	-3.36	216.2	0	20.93

Table A.3. Strength parameters in strain space (dimensionless)(- see [4] for formulae for calculating these quantities from the F-values).

Material	G_{xx}	G_{yy}	G_{xy}	G_{ss}	G_x	G_y
E-glass epoxy	790.302	11712.24	1590.64	2746.29	23.383	77.276
S-glass epoxy	1068.7	18291.07	2851.65	10009.67	84.7494	244.564
Graphite-epoxy	12004	10680	-3069	11117	60.64	216.5

Table A.4. Engineering constants and specific gravity.

Material	E_x (GPa)	E_y (GPa)	υ_{xy}	υ_{yx}^*	E_s (GPa)	Sp. gr.
E-glass epoxy	11.69	19.03	0.42144	0.68613	11.8354	1.8
S-glass epoxy	58.07	13.793	0.293	0.067	5.31	1.7
Graphite-epoxy	181	10.3	0.28		7.17	1.6

*Note: $\upsilon_{xy}/E_x = \upsilon_{yx}/E_y$.

(B) Specific gravity (s.g.) of transported fluids

Table B.1. Specific gravities of selected fluids.

Fluid	Specific gravity (s.g.)
Water	1.0
Crude oil	0.9
Natural gas	0.005

(C) Selected pipe geometries

Table C.1. Sample pipe geometries for oil and gas transportation.

Application	Nom. Diam., D (in)	Wall thick., h (in)	D/h range (typical)
Flowlines (F/L)	4, 6, 8	1/8, 1/4	16 - 64
Delivery lines (D/L)	10, 14, 16	1/4, 1/2	20 - 64
Trunk lines (T/L)	18, 20, 24	1/2 - 1	18 - 48
Loading lines (L/L)	30, 40, 50	1, 1.5	20 - 50

Appendix III: Comparison of computed values of L_{opt} with those of another model in double columns

A. Comparison for a wide range of pipe diameters (using h=3/8").

D (mm)	D/h	p @ max.*	Lopt (m) graphite epoxyL-interact	L-shear	Lopt (m) E-glass epoxy L-interact	L-strain	Lopt (m)L-sys.des.*
100	10.49869	19.05	4.615	4.0223	2.87876	2.3208	3.5
150	15.74803	12.7	5.8684	5.111	3.657	2.948	3.9
200	20.99738	9.525	6.923	6.0258	4.3105	3.47473	4.2
250	26.24672	7.62	7.85	6.8233	4.883	3.937	4.5
300	31.49606	6.35	8.687	7.5454	5.4	4.3526	4.7
350	36.74541	5.443	9.4553	8.2086	5.872	4.7342	4.8
400	41.99475	4.7625	10.17	8.819	6.3106	5.0873	4.8
450	47.24409	4.233	10.8423	9.393	6.7216	5.42	4.8
500	52.49344	3.81	11.478	9.9362	7.11	5.732	4.9
550	57.74278	3.4636	12.083	10.448	7.478	6.02915	4.9
600	62.99213	3.175	12.662	10.9422	7.829	6.313	4.9

*For maximum hoop stress of 10 MPa, see [3].

B. Comparison for flowline pipes.

D (mm)	h (in)	D/h	p @ max.*	Lopt (m) Graphite epoxy L-interact L-shear	Lopt (m) E-glass epoxy L-interact L-strain	Lopt (m)L-sys.des.*
40	0.25	6.30	31.75	2.481	1.55	2.7
50	0.25	7.87	25.40	2.854	1.782	2.9
80	0.25	12.60	15.88	3.796	2.368	3.3
100	0.25	15.75	12.70	4.327	2.698	3.5
150	0.25	23.62	8.47	5.455	3.397	3.9
200	0.25	31.50	6.35	6.402	3.983	4.2

*For maximum hoop stress of 10 MPa, see [3].